Coordinated Control of a Wind Turbine Array
for Power Maximization

Eilyan Bitar and Pete Seiler

Abstract—Wind turbines are currently operated at their peak
power extraction efficiency without consideration of the aero-
dynamic coupling between neighboring turbines. This mode of
operation leads to inefficient, sub-optimal power capture at the
wind farm level. By explicitly accounting for the aerodynamic
wake interactions between neighboring wind turbines within
a farm, we aim to characterize optimal control policies that
maximize the power captured by a collection of wind turbines
operating in quasi-steady wind flow conditions. In this paper, we
consider two wake interaction models, termed *near-field* and *far-
field*, describing wake propagation under densely and sparsely
spaced turbine arrays, respectively. Under the near-field model,
we derive a closed form expression for the optimal control policy
maximizing power capture for a one-dimensional array of wind
turbines. Moreover, we show that the optimal control policy is
both static and independent of the free stream wind velocity,
being thus amenable to a decentralized implementation. We
also formulate and solve numerically the problem of jointly
optimizing over the control policy and placement of turbines in
a one dimensional 3-turbine array under the far-field model.

Index Terms—Wind Energy, Optimal Control.

I. INTRODUCTION

Concerns over energy security and global warming have
manifested in a dramatic growth in the rate of installed
wind power capacity in the United States [1], and world-
wide [7], over the last decade. However, because of the
signficant capital cost of wind turbine infrastructure and the
attendant variability in power supply, wind integration today
has relied heavily on subsidies and extra-market support to
sustain its economic viability. Common examples include
investment and production credits, feed-in tariffs, mandated
purchases, and variability cost exemption – the last of which
is commonly socialized amongst the load serving entities
(LSE) within a common control area. The practice of pushing
the cost of additional reserves, needed to firm wind, on
to the LSEs will become financially unsupportable as the
penetration of wind increases under the current operating
paradigm. In fact, a recent study by NREL predicts that
regulating reserve requirements in the PJM interconnection

will increase, on average, by 1500 MW under a 20% percent
wind energy penetration scenario [6].

As a result, new policies and market-based solutions,
placing greater responsibility on wind power producers, are
being developed to facilitate the integration of wind at levels
of increased penetration approaching 10-20%. For example,
the *Dispatchable Intermittent Resource* program initiated by
the Midwest Independent System Operator treats wind farms
as dispatchable generators required to operate within certain
limits outside of which they face penalties for deviation [18].
Additionally, the California Independent System operator
is developing a new *Flexible Ramping* product aimed at
compensating inter-interval ramps in net demand ($\approx$ load
minus non-dispatchable resources) – the cost of which will
be allocated to those parties responsible for its procurement
[25]. Both of these programs essentially impose a variability
cost on the wind power producer. This creates an incentive to
the wind farm to firm its output, which manifests in a trade-
off between power maximization and variability mitigation.
Clearly, improving the viability of wind in this changing
regulatory landscape will require technical innovations that
enable a balance of these two objectives.

In this paper, we focus on the problem of wind farm
power maximization, as this is essential to maximizing the
revenue derivable from production tax credits and feed-in
tarrifs under the current regulatory environment. Tradition-
ally, wind farms are controlled in a decentralized fashion,
where each turbine is operated to maximize power extraction
locally, without consideration of aerodynamic interactions
between neighboring turbines within a farm. Essentially, this
amounts to a greedy control policy where each turbine i
is operated at its peak efficiency according to Betz' Law
[5]. In practice however, the energy extracted from the
free stream flow at a leading turbine will generate a wake
with reduced energy content, thereby mitigating the power
extractable by nearby downstream turbines. Many papers [2],
[4], [9], [12], [13], [16], [15], [17], [19], [22], [20], [21],
[24] have recently shown that maximizing power capture
at the individual turbine level leads to sub-optimal power
capture at the farm level. Clearly, optimized placement of
and increased spatial separation between turbines can limit
aerodynamic interactions and thus improve the farm level
power capture under the greedy policy – a topic which has
received significant attention in recent years [23].

There have been several papers in the recent literature that
have explored this question from different angles. In [9],
Johnson et al. present several simulation based results demon-

strating sub-optimality in power capture when individual turbines are operated at their peak efficiencies. Marden et al. [16], [15] dispense with the challenge of explicitly modeling aerodynamic interactions between neighboring turbines and rely instead on a game-theoretic learning approach to solve the control problem. The approach does not require an explicit model of the aerodynamic interactions. However, the achievable performance may be limited in practice if the wind velocity varies more rapidly than the time required to converge to the optimal policy. In [13], the authors present a novel control-oriented model to characterize wake interactions between neighboring turbines and demonstrate through simulation the improvement in farm-level power capture when coordinating the control actions of the individual turbines. In [23], Tzanos et al. propose the use of a randomized algorithm to optimize the placement of wind turbines within a fixed area to maximize total power capture. While the authors' proposed algorithm improves upon the performance of conventional genetic algorithms used for turbine siting, the problem formulation assumes a fixed control policy and hence does not explore the gains achievable through the co-optimization of turbine placement and control.

In the present paper, we build on the problem formulation and numerical results of [9] by deriving a closed form expression for the optimal control policy maximizing power capture for a one-dimensional array of densely spaced wind turbines. Under quasi-steady conditions, the optimal control policy is shown to be static and independent of the free stream wind velocity, being thus amenable to a decentralized implementation. We also formulate and solve numerically the problem of jointly optimizing over the control policy and turbine placement to maximize power capture of a one dimensional 3-turbine array. We do not consider the problem of load mitigation in this paper, as this is left for future work.

In Section II, we present a model for power capture at an individual turbine based on actuator disk theory and describe a general wake generation and interaction model to characterize the aerodynamic coupling between neighboring turbines within a farm. Modeling of turbine wake interactions remains an active research area and hence two different wake models, named *near-field* and *far-field*, are described. In Sections III and IV, we present results characterizing an optimal control policy that results in farm level power maximization under the near-field and far-field wake interaction models, respectively. Finally, we close with conclusions and suggestions for future research directions in Section V. The majority of proofs are omitted due to space constraints – with the exception of the primary results, whose proofs are located in the appendix.

II. PROBLEM FORMULATION

This section presents the wind farm model used in this paper. Consider a one dimensional array of N identical wind turbines as shown in Figure 1. Turbine i is located downstream of turbine 1 by a distance x_i. The air flow

velocity upstream of turbine 1 is assumed to be uniform with speed defined as v_∞. It is further assumed that all turbines are perfectly aligned with the direction of the upstream airflow, such that the air flow is orthogonal to each turbine's plane of rotation. The power generated by the wind farm depends on the free-stream wind speed and the control actions of each turbine. In the following subsections, we describe the model of the wind farm power generation process.
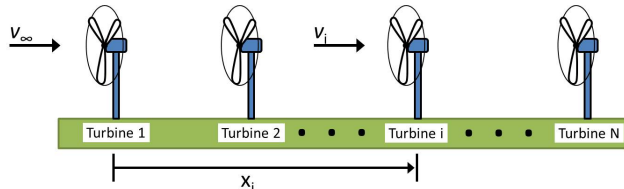

Fig. 1.   One-dimensional array of turbines.

A. Turbine Power Capture

The power captured by turbine i is given by

$$P_i(a_i, v_i) = \frac{1}{2}\rho A v_i^3 C_P(a_i) \tag{1}$$

where ρ is the air density, A is the area swept by the turbine blades, and v_i is the average "inlet" wind speed for turbine i [5], [14]. The non-dimensional power coefficient C_P is the fraction of the available wind power captured by the turbine. C_P depends on the macroscopic aerodynamic properties of the turbine. A simple expression for the power coefficient can be derived using actuator disk theory [5], [14] as follows. Define the axial induction factor, a_i, as the relative decrease in velocity from the inlet to the rotor plane, i.e. $a_i := (v_i - v_{rotor,i})/v_i$. The dependence of the power coefficient on the induction factor is given by actuator disk theory as:

$$C_P(a_i) = 4a_i(1 - a_i)^2 \tag{2}$$

The induction factor is treated as the turbine control input in this model. Equation 2 leads to Betz' Law: the efficiency for a turbine is bounded by $C_P(a_i) \leq \frac{16}{27} \approx 0.59$ with the bound achieved by operating at $a_i = \frac{1}{3}$. A key point is that the induction factor $a_i = \frac{1}{3}$ maximizes power capture for a single turbine, but need not be optimal for an array of turbines due to the aerodynamic interactions between neighboring turbines. The axial thrust force also depends on the induction factor: $T(a_i, v_i) = \frac{1}{2}\rho A v_i^2 C_T(a_i)$ where $C_T(a_i) = 4a_i(1 - a_i)$ is the non-dimensional thrust coefficient. Thus the axial induction factor affects both the captured power as well as the thrust loads on the turbine.

Equations 1 and 2 form a simplified model of the power capture characteristics for a single turbine. The actual control inputs on a utility scale turbine are the blade pitch angles and generator torque. In addition, higher fidelity models, e.g. the FAST simulation package developed by the National Renewable Energy Laboratory [10], include more detailed

models of the aerodynamic forces and structural (tower, blade, gearbox) flexibilities. As noted above, this paper treats the axial induction factor a_i as the turbine control input. The induction factor computed for each turbine would need to be converted to blade pitch angles and generator torques for an implementation on an actual turbine.

B. Wake Interaction Model

The actions of a single turbine disrupt the freestream velocity and lead to wake effects downstream of the turbine. Consider the effect of turbine 1 on the flow at a downstream distance x and spanwise distance s behind the turbine. The velocity at location (x, s) is given by:

$$v(x, s, a_1) = v_\infty \left(1 - \delta v(x, s, a_1)\right), \tag{3}$$

where $\delta v(x, s, a_1)$ is the relative velocity deficit with respect to the free-stream velocity v_∞ induced by the control action, a_1, of turbine 1. As a concrete example, the Park Model [8], [11], [9], [16], [2] defines the relative velocity deficit as:

$$\delta v(x, s, a_i) := \begin{cases} 2a_i \left(\frac{D}{D + 2k_r x}\right)^2 & \text{if } s \leq \frac{D + 2k_r x}{2} \\ 0 & \text{else} \end{cases}, \tag{4}$$

where D is the turbine rotor diameter and k_r is a roughness constant that determines the wake expansion. An alternative model for the relative velocity deficit uses a power law and Gaussian wake dependence on the downstream and spanwise directions, respectively [4], [20], [21].

The average inlet speed at turbine 2 is affected by operating in the wake of turbine 1. A simple coupling relation between turbines 1 and 2 can be derived for a wide class of relative velocity deficit functions $\delta v(x, s, a_1)$. Assume the relative velocity deficit behind turbine 1 is a linear function of the induction factor: $\delta v(x, s, a_1) = \kappa(x, s)a_1$ for some function $\kappa(x, s)$. Turbine 2 is located downstream of turbine 1 by a distance x_2. The average inlet velocity for turbine 2 is:

$$v_2 = \frac{1}{A} \int_A v_\infty (1 - \delta v(x_2, s, a_1)) dA \tag{5}$$

Defining $\kappa_{1,2} := \frac{1}{A} \int_A \kappa(x_2, s) dA$ yields

$$v_2 = v_\infty (1 - \kappa_{1,2} \cdot a_1), \tag{6}$$

where $\kappa_{1,2}$ is the coupling constant that relates the control action of turbine 1 to the decrease in average wind speed incident at turbine 2. This is a quasi-steady state model with a linear relation between the induction factor and the downstream inlet velocity. The coupling constant $\kappa_{1,2}$ aggregates all of the information about the array geometry (separation distance) and relative velocity deficit model for the wake. The integral in the coupling constant averages the relative velocity deficit over the rotor plane of turbine 2. A weighted integral over the rotor plane would lead to the same form as in Equation 6. Finally, a reasonable characteristic for a wake model is that the far downstream velocity converges to the free-stream velocity, i.e. $\delta v(x, s, a_1) \to 0$ as $x \to \infty$.

It follows immediately that $\kappa_{1,2} \to 0$ as $x_2 \to \infty$ for velocity deficit models with this "far-field" behavior.

The coupling relation in Equation 6 can be extended to the case of more than two turbines. Two specific models will be used in this paper. First, a *far-field* model is defined as

$$v_i = v_\infty \left(1 - \sum_{j=1}^{i-1} \kappa_{j,i} \cdot a_j\right), \tag{7}$$

for $i = 2, \ldots, N$ and $v_1 = v_\infty$. This model assumes a linear superposition of wake velocity deficits. One drawback of this model is that it can result in unrealistic negative inlet velocities for some induction factors and coupling constants. Nonlinear relations, e.g. a Euclidean norm relation, have also been proposed [16] for superposition of multiple wakes. Equation 7 is termed a far-field model, because it satisfies $v_i \to v_\infty$ as $x_i - x_{i-1} \to \infty$. Specifically, $v_i \to v_\infty$ if the relative velocity deficit model satisfies $k_{j,i} \to 0$ ($j = 1, \ldots, i-1$) as the spacing between turbines i and $i - 1$ increases.

A *near-field* model will also be considered in this paper:

$$v_i = v_{i-1} \left(1 - \kappa_{i-1,i} a_{i-1}\right), \tag{8}$$

for $i = 2, \ldots, N$ and $v_1 = v_\infty$. In this model, the control action of turbine $i - 1$ only directly affects the inlet velocity of turbine i. However, the control action of turbine $i - 1$ indirectly affects all downstream turbines $(i, i + 1, \ldots, N)$ through the one-step velocity deficit relation defined in Equation 8. This near-field model satisfies $v_i \to v_{i-1}$ as turbine i moves farther downstream from turbine $i - 1$, i.e. the freestream velocity is not recovered far downstream. Although the far-field model is the more common model in the literature, the near-field model may prove to be more appropriate for closely spaced turbines. This is a conjecture that needs to be verified with empirical analysis.

C. Power Maximization

The joint axial induction factor for the turbine array is $a = (a_1, \cdots, a_N) \in \mathcal{A}$ where the allowable set of induction factors is $\mathcal{A} = [0, \frac{1}{3}]^N$. The total power extracted from the array of turbines operating under a joint axial induction factor $a \in \mathcal{A}$ is given by

$$J(a, v_\infty) = \sum_{i=1}^{N} P_i(a_i, v_i) \tag{9}$$

Note that the power generated by turbine i depends on the actions of all upstream turbines via the inlet velocity $v_i := v_i(v_\infty, a_1, \ldots, a_{i-1})$. A joint axial induction factor a° is said to be *optimal* if it satisfies

$$a^\circ \in \arg\max_{a \in \mathcal{A}} J(a, v_\infty). \tag{10}$$

Here, we assume that the supremum of J is achieved. Computing an optimal solution is nontrivial as the objective function J is, in general, not concave in a. Moreover, in

solving problem (10), we seek optimal induction factors parameterized as explicit functions of their corresponding inlet conditions. With a slight abuse of notation we denote this dependence by $a_i = a_i(v_i)$.

III. RESULTS: NEAR-FIELD

In this section, we explore the problem of maximizing power capture under the *near-field* wake interaction model in Equation 8. Given this spatially causal relationship characterizing the dependence structure between inlet velocities across turbines, it is straightforward to show that the *principle of optimality* [3] is satisfied by problem (10), i.e. given an optimal policy $a^\circ = (a_1^\circ, \cdots, a_N^\circ)$ parameterized by the inlet wind speed $v_1 = v_\infty$, it holds that $(a_i^\circ, \cdots, a_N^\circ)$ is also optimal for the sub-problem parameterized by the intermediary inlet wind speed, v_i. We thus consider a dynamic programming (DP) approach to enumerating an optimal policy.

In the customary DP fashion, define the inlet speed v_i and induction factor a_i as the *state* and *control input*, respectively, of turbine i. The *state transition function* is given by the near-field relation (8). For any policy $a \in \mathcal{A}$, the *cost-to-go* at turbine i with inlet speed $v_i = v$ is defined as

$$J_i(a, v) = \sum_{j=i}^{N} P_j(a_j, v_j). \qquad (11)$$

Let $\mathcal{A}_i$ denote the allowable induction factors for turbine i. This notation is defined for generality, but in many cases the allowable induction factors will simply be $\mathcal{A}_i = [0, \frac{1}{3}]$. It follows that the *value function* for a given inlet speed $v_i = v$ at turbine i is defined as

$$J_i^\circ(v) = \max_{a \in \mathcal{A}^{(i)}} J_i(a, v), \qquad (12)$$

where $\mathcal{A}^{(i)} = \prod_{j=i}^{N} \mathcal{A}_j$ is the set of allowable induction factors for turbines i through N.

Lemma III.1 (Bellman equation). *The value function satisfies the following backward iteration. Given an inlet wind speed $v_N = v$ at the terminal turbine N,*

$$J_N^\circ(v) = \max_{a \in \mathcal{A}_N} P_N(a, v) \qquad (13)$$

and for $1 \le i \le N - 1$ with inlet wind speed $v_i = v$ at turbine i,

$$J_i^\circ(v) = \max_{a \in \mathcal{A}_i} \left\{ P_i(a, v) + J_{i+1}^\circ(v(1 - a \, \kappa_{i,i+1})) \right\}. \qquad (14)$$

The proof of Lemma III.1 follows directly from the principle of optimality. This has a DP "cost-to-go" interpretation that can be restated as: the maximal power produced by turbines i through N is obtained by maximizing the sum of the power produced by turbine i and the power produced by the remaining turbines operating optimally in the wake of turbine i. Further refinement of the value function yields the following simplified form, which reveals state independence

of the optimal policy. Without loss of generality, assume identical swept rotor areas, $A_i = A$ for all turbines i.

Lemma III.2 (State independent decisions). *The value function satisfies the following backward iteration for $1 \le i \le N$.*

$$J_i^\circ(v) = cv^3 \max_{a \in \mathcal{A}_i} \left\{ a(1 - a)^2 + (1 - a \, \kappa_{i,i+1})^3 \phi_{i+1} \right\}, \qquad (15)$$

where

$$\phi_i = (1 - a_i^\circ \kappa_{i,i+1})^3 \phi_{i+1} + a_i^\circ (1 - a_i^\circ)^2 \qquad (16)$$

and $\phi_{N+1} = 0$, $\kappa_{N,N+1} = 0$, and $c = 2\rho A$.

Remark III.3. *Lemma III.2 characterizes the value function as a simple recursive procedure to compute the optimal policy a°, which is shown to be independent of the system state, i.e. it is independent of the turbine inlet velocity v.*

Theorem III.4 (Optimal policy). *For $1 \le i \le N$, let $\phi = \phi_{i+1}$ and $\kappa = \kappa_i$.*

$$a_i^\circ = \frac{1}{3} \left(\frac{2 - 3\phi\kappa^2 - \sqrt{1 - 12\phi\kappa^2 + 9\phi\kappa + 3\phi\kappa^3}}{1 - \phi\kappa^3} \right) \qquad (17)$$

where ϕ_{i+1} satisfies the backward iteration specified by (16).

Theorem III.5 (Optimal policy, $\kappa_{i,i+1} = 2$). *For $1 \le i \le N$, let $\kappa_i = 2$.*

(a) The optimal policy is given by

$$a_i^\circ = \frac{1}{2(N - i) + 3}. \qquad (18)$$

(b) The power extracted by the ith turbine under the optimal policy a° is given by

$$P_i(a_i^\circ, v_i) = \frac{1}{2}\rho A v_\infty^3 16 \frac{(N - i + 1)^2}{(2N + 1)^3}.$$

(c) The total power extracted by the wind farm under a° is

$$J(a^\circ, v_\infty) = \frac{1}{2}\rho A v_\infty^3 \frac{8N(N + 1)}{3(2N + 1)^2},$$

whose limit as the number of turbines goes to infinity, is

$$J_\infty := \lim_{N \to \infty} J(a^\circ, v_\infty) = \frac{1}{2}\rho A v_\infty^3 \frac{2}{3}.$$

Theorem III.5 provides a closed form expression for the numerical results corresponding to the two-turbine example presented in [9].

Remark III.6 (Improvement on the greedy policy). *According to Theorem III.5, the peak aggregate power capture efficiency of an infinite array of densely spaced turbines is given by of $C_P^\circ = 2/3$. Under the greedy policy ($\overline{a}_i = 1/3$ for all i), one can readily show that the power captured by an N-turbine array is given by*

$$J(\overline{a}, v_\infty) = \frac{1}{2}\rho A v_\infty^3 \left(\frac{16}{26}\right) \left(1 - \left(\frac{1}{27}\right)^N\right),$$

whose limit yields an aggregate power capture efficiency of $\overline{C}_P = 16/26$. *Thus, operating the wind turbine array under the optimal policy* a° *yields an improvement of*

$$\frac{C_P^\circ - \overline{C}_P}{\overline{C}_P} = 8.33\%.$$

IV. RESULTS: FAR-FIELD

This section focuses on a three turbine array using the far-field model. This builds on the prior examination of the three turbine array in [9]. Assume the turbine locations (x_2, x_3) are given. Under the far-field model described in Section II, the power generated by the three turbine array is

$$P(a_1, a_2, a_3) = \frac{1}{2}\rho A \left(v_1^3 C_P(a_1) + v_2(a_1)^3 C_P(a_2) \right. \quad (19)$$
$$\left. + v_3(a_1, a_2)^3 C_P(a_3) \right)$$

The far-field wake interaction model (Equation 7) gives the turbine inlet velocities:

$$v_1 = v_\infty \quad (20)$$
$$v_2(a_1) = v_\infty(1 - \kappa_{1,2}a_1) \quad (21)$$
$$v_3(a_1, a_2) = v_\infty(1 - \kappa_{1,3}a_1 - \kappa_{2,3}a_2) \quad (22)$$

The joint axial induction factor for the three turbine array is $a = (a_1, a_2, a_3) \in \mathcal{A} := [0, \frac{1}{3}]^3$. The objective is to find the optimal joint induction factor that satisfies

$$a^\circ \in \arg\max_{a \in \mathcal{A}} P(a_1, a_2, a_3). \quad (23)$$

The induction factor $a = \frac{1}{3}$ maximizes the power capture for a single turbine operating in isolation. However, operating each turbine in the array at this induction factor, i.e. $a_i = \frac{1}{3}$, does not yield the maximal combined power from the array [9]. In particular, maximizing the power capture of the leading turbines in the array leaves less energy to be captured by the trailing turbines. Thus the joint power produced by the array $P(a_1, a_2, a_3)$ can be increased by operating some turbines away from the peak efficiency induction factor.

If all wake interaction coupling constants $\kappa_{i,j}$ are zero then it can be shown that the Hessian $\nabla^2 P$ is strictly negative definite on $\mathcal{A}$. It follows by continuity that P is a concave function for sufficiently small coupling constants. For general coupling constants, however, P is not a concave function. Hence the optimization in Equation 23 may have multiple local optima. One concrete statement is that $a_3^o = \frac{1}{3}$ is required for global optimality. In other words, the last turbine in the array should maximize its power capture because there are no subsequent turbines operating in its wake.

The power maximization problem was solved for the three turbine array by gridding on the space of induction factors. As noted above, turbine 3 must operate at peak efficiency ($a_3^o = \frac{1}{3}$) and hence the gridding was performed on a two-dimensional space $(a_1, a_2) \in [0, \frac{1}{3}]^2$. The calculations were performed assuming equally spaced turbines: $x_2 - x_1 = x_3 - x_2 := x$. In addition, the Park Model (Equation 4) was used to compute the coupling constants.

The integrations needed to compute the coupling constants simplify considerably because the relative velocity deficit is constant within the wake region for the Park Model. The coupling constants become $\kappa_{1,2} = \kappa_{2,3} = 2\frac{D^2}{(D+2k_r x)^2}$ and $\kappa_{1,3} = 2\frac{D^2}{(D+4k_r x)^2}$. Finally, the rotor diameter and roughness constants were chosen as $D = 100$m and $k_r = 0.075$. Figure 2 shows the optimal induction factor for turbine 2, a_2^o, as a function of the turbine separation distance, x. As discussed above, the optimal input for turbine 2 is not equal to the peak efficiency for a single turbine, $a_2^o \neq \frac{1}{3}$. As the turbine separation increases the wake interactions decrease and the optimal induction factor for turbine 2 converges to the peak efficiency point, $a_2^o \to \frac{1}{3}$ as $x \to \infty$. Note that for separations less than 2 rotor diameters the optimal point corresponds to shutting down turbine 2, $a_2^o = 0$. In other words there is no benefit to installing densely spaced turbines, according to the Park wake model. It would be interesting to verify this result with a high fidelity simulation.
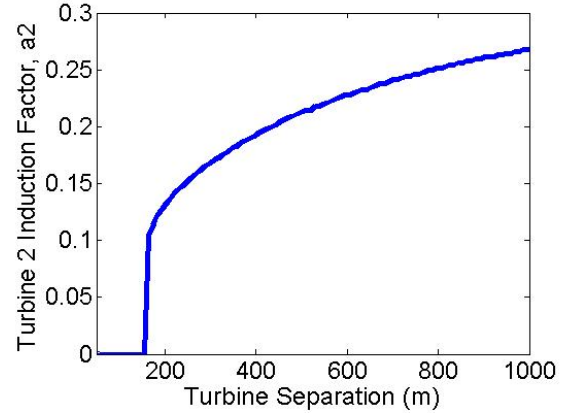

Fig. 2. Optimal induction factor for turbine 2 vs. turbine spacing.

A natural question follows: given a fixed length budget L for a one dimensional array, how should the turbines be spaced to maximize the total power generated by the array? This optimization is related to the real-world task of micro-siting of turbines, with the additional complexity of optimizing over both the operating induction factors and the turbine placement. To simplify the problem, notice that turbines 1 and 3 must be separated by the given distance L, i.e. $x_3 = L$. This follows because the coupling constants are inversely related to separation distance and decreasing any coupling constant (all else being equal) will increase the generated power. Let $P(a, x_2)$ denote the power generated by the three turbine array at the joint induction factor $a \in \mathcal{A} := [0, \frac{1}{3}]^3$ and with turbine 2 located at x_2. The problem is to co-optimize over the joint induction factor, a, and turbine 2 location, x_2, for a given array length L.

$$(a^\circ, x_2^\circ) \in \arg\max_{a \in \mathcal{A}, 0 < x_2 < L} P(a, x_2) \quad (24)$$

The coupling constants are computed using the Park Model with $D = 100$m and $k_r = 0.075$. The location of x_2

enters the optimization via the calculation of the coupling constants $\kappa_{1,2}$ and $\kappa_{2,3}$. This optimization was solved on a grid of (a_1, a_2, x_2) with $a_3^\circ = \frac{1}{3}$. Figure 3 shows the optimal power versus the array length. The optimal power on the vertical axis is normalized by $\frac{3}{2}\rho A v_\infty^3 C_P(\frac{1}{3})$. This normalization factor is the power captured by three turbines in isolation operating at their peak efficiency. As expected, the normalized optimal power shown in Figure 3 converges to one as array length tends to infinity. For finite lengths, the three turbine array generates less energy (for any placement and induction factor) than three turbines operating at peak efficiency in isolation. Using the Park wake model, one still experiences 20% loss in power at an array length of 20 rotor diameters. This roughly corresponds to a 10 rotor diameter spacing between the turbines. Figure 4 shows the optimal placement of turbine 2 versus the array length. The optimal placement is specified as a fraction of the array length, i.e. the vertical axis is $x_2^\circ(L)/L$. This plot shows some numerical artifacts of the gridding procedure. Qualitatively, the plot shows that the second turbine should be placed slightly closer to turbine 3 than to turbine 1. At very low array lengths L, the placement of turbine 2 becomes immaterial, because according to Figure 2, the optimal solution is $a_2^\circ = 0$ for $L < 175$ m.
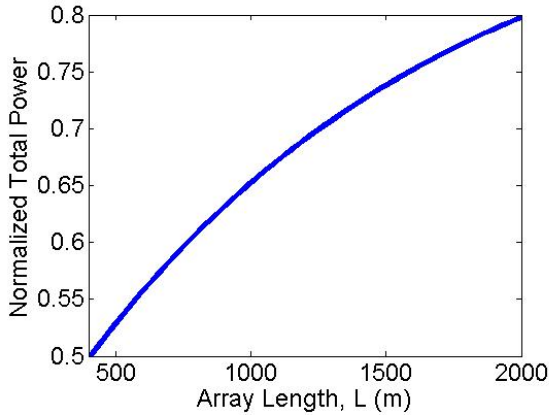
Fig. 3.   Optimal power (normalized) vs. array length.

V. CONCLUSION

In this paper, we've explored the problem of farm-level power maximization under two different quasi-steady state wake interaction models. First, the principle of optimality was used to derive a closed-form expression for the optimal turbine control policy using a near-field model. Second, the joint optimization over the control policy and turbine placement was numerically solved for a three turbine array under a far-field wake model. Development of simplified, control-oriented models of the turbine interactions within a wind farm is still an ongoing endeavor. Thus these results should be validated on higher fidelity wind farm models. Finally, as this paper focused exclusively on power maximization, future work will also consider the problem of load reduction.
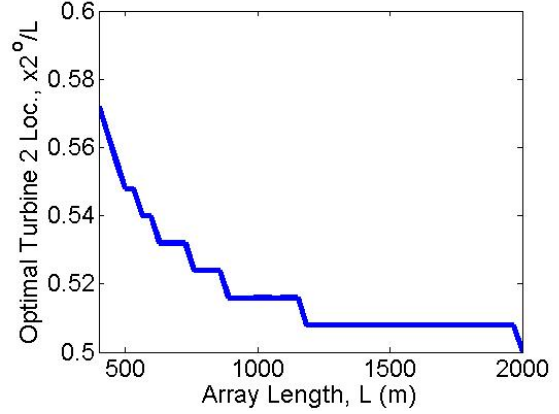
Fig. 4.   Optimal power (normalized) vs. array length.

APPENDIX

A. Proof of Lemma III.2

The result is proven by induction. The base case, $i = N$, follows directly from inspection of the terminal value function (13). For the inductive step, assume Equation (15) holds for stage i. Direct application of the induction hypothesis to the Bellman equation (14) at stage $i-1$ gives us

$$J_{i-1}^\circ(v) = \max_{a \in \mathcal{A}_{i-1}} \left\{ cv^3 a(1-a)^2 + cv^3(1-a\kappa_{i-1,i})^3 \phi_i \right\},$$
$$= cv^3 \max_{a \in \mathcal{A}_{i-1}} \left\{ a(1-a)^2 + (1-a\kappa_{i-1,i})^3 \phi_i \right\},$$

where $\phi_i = (1 - a_i^\circ \kappa_{i,i+1})^3 \phi_{i+1} + a_i^\circ(1 - a_i^\circ)^2$. ∎

B. Proof of Theorem III.5

Part (a). The result is proven by induction on the statements

$$a_i^\circ = \frac{1}{2(N-i)+3}, \tag{25}$$

$$\phi_i = \frac{1}{6}\left(1 - \frac{1}{(2(N-i+1)+1)^2}\right). \tag{26}$$

First notice that under the assumption, $\kappa_{i,i+1} = 2$ for all i, the expression for a_i° in Theorem III.4 simplifies to

$$a_i^\circ = \frac{1}{3}\left(\frac{2 - 12\phi_{i+1} - \sqrt{1 - 6\phi_{i+1}}}{1 - 8\phi_{i+1}}\right), \tag{27}$$

where $\phi_i = (1 - 2a_i^\circ)^3 \phi_{i+1} + a_i^\circ(1 - a_i^\circ)^2$.

Base step. The base case, $i = N$, follows directly from the boundary condition $\phi_{N+1} = 0$.

Induction step. Now, assume that Equations (25) and (26) hold for stage $i+1$. Direct substitution of the closed form expression for ϕ_{i+1} into Equation (27) yields

$$a_i^\circ = \frac{\frac{2}{(2(N-i)+1)^2} - \frac{1}{(2(N-i)+1)}}{\frac{4}{(2(N-i)+1)^2} - 1}.$$

Straightforward algebraic manipulations reveal the desired form $a_i^\circ = 1/(2(N-i)+3)$. Similarly, substitution of the explicit expressions for (a_i°, ϕ_{i+1}) into the difference equation for ϕ_i yields, after simple algebraic manipulations, the desired form of ϕ_i – thus, completing the inductive step.

Parts (b)-(c). Recall Equation (1) for the definition of power extracted at a single turbine i as a function of the inlet velocity v_i and induction factor a_i. Direct substitution of the optimal policy a_i° into the power efficiency coefficient C_p yields

$$C_p(a_i^\circ) = 16 \frac{(N-i+1)^2}{(2(N-i)+3)^3}.$$

Iterating Equation (8) for the inlet velocity v_i back to the boundary condition $v_1 = v_\infty$ and substituting for the optimal policy gives

$$v_i = v_\infty \prod_{k=1}^{i-1} (1 - 2a_k)$$
$$= v_\infty \prod_{k=1}^{i-1} \frac{2(N-k)+1}{2(N-k)+3} = v_\infty \frac{2(N-i+1)+1}{2(N-1)+3},$$

where the last equality follows from cancellation of intermediate terms in the product. Using these expressions, one can write the total power extracted by N turbines under the optimal policy a° as

$$\frac{J(a^\circ, v_\infty)}{8\rho A v_\infty^3} = \sum_{i=1}^{N} \left(\frac{2(N-i)+3}{2N+1} \right)^3 \frac{(N-i+1)^2}{(2(N-i)+3)^3}$$
$$= \sum_{i=1}^{N} \frac{(N-i+1)^2}{(2N+1)^3},$$

which can be expanded as

$$\frac{J(a^\circ, v_\infty)}{8\rho A v_\infty^3} = \frac{N(N+1)^2}{(2N+1)^3} + \frac{1}{(2N+1)^3} \sum_{i=1}^{N} i^2 - 2(N+1)i.$$

Using closed form expressions for the summation of the first N natural numbers (e.g., $1+2+\cdots+N = N(N+1)/2$) and their squares (e.g., $1^2+2^2+\cdots+N^2 = N(N+1)(2N+1)/6$), it is straightforward to show that

$$\frac{J(a^\circ, v_\infty)}{8\rho A v_\infty^3} = \frac{N(N+1)}{6(2N+1)^2},$$

whose limit yields the desired result. ∎

REFERENCES

[1] American Wind Energy Association. AWEA U.S. Wind Industry: First quarter 2012 market report. http://www.awea.org/learnabout/publications/reports/, 2012.
[2] AWSTruepower. Openwind: Theoretical basis and validation, 2010.
[3] R.E. Bellman. *Dynamic Programming*. Princeton University Press, 1957.
[4] A. J. Brand and M. Soleimanzadeh. Two control solutions for wind farm management and operation on the grid. In *EWEA Offshore Conference*, 2011. ECN-M-11-109.
[5] T. Burton, D. Sharpe, N. Jenkins, and E. Bossanyi. *Wind Energy Handbook*. John Wiley & Sons, 1st edition, 2001.
[6] EnerNex Corp. Eastern wind integration and transmission study, 2011. Report NREL/SR-550-47078.
[7] Global Wind Energy Council. GWEC global statistics: Global cumulative installed capacity 1996-2011. http://www.gwec.net/global-figures/graphs/, 2012.
[8] N.O. Jensen. A note on wind generation interaction. Technical report, Risø, 1983. Risø-M-2411.
[9] K.E. Johnson and N. Thomas. Wind farm control: addressing the aerodynamic interaction among wind turbines. In *American Control Conference*, pages 2104–2109, 2009.
[10] J.M. Jonkman and M.L. Buhl. *FAST User's Guide*. National Renewable Energy Laboratory, Golden, Colorado, 2005.
[11] I. Katic, J. Højstrup, and N.O. Jensen. A simple model for cluster efficiency. In *Proceedings of the European Wind Energy Conference*, pages 407–410, 1986.
[12] M. Kristalny and D. Madjidian. Decentralized feedforward control of wind farms: prospects and open problems. In *Conference on Decision and Control and European Control Conference*, pages 3464–3469, 2011.
[13] D. Madjidian and A. Rantzer. A stationary turbine interaction model for control of wind farms. In *IFAC World Congress*, pages 4921–4926, 2011.
[14] J.F. Manwell, J.G. McGowan, and A.L. Rogers. *Wind Energy Explained: Theory, Design, and Application*. Wiley, 2010.
[15] J. R. Marden, S. D. Ruben, and L. Y. Pao. A model-free approach to wind farm control using game theoretic methods. *Submitted for journal publication*, 2012.
[16] J. R. Marden, S. D. Ruben, and L. Y. Pao. Surveying game theoretic approaches for wind farm optimization. In *Proceedings of the AIAA Aerospace Sciences Meeting*, 2012.
[17] P.F. Odgaard, M.A.B. Baekgaard, and B. Astrup. Model based control of wind parks. In *EWEC Conference*, 2010.
[18] Midwest Independent Transmission System Operator. Electric tariff filing designating dispatchale intermittent resources, 2010. Filed with the Federal Energy Regulatory Commission.
[19] L.Y. Pao and K.E. Johnson. A tutorial on the dynamics and control of wind turbines and wind farms. In *American Control Conference*, pages 2076–2089, 2009.
[20] M. Soleimanzadeh, A. J. Brand, and R. Wisniewski. A wind farm controller for load and power optimization in a farm. In *IEEE International Symposium on Computer-Aided Control System Design*, pages 1202–1207, 2011.
[21] M. Soleimanzadeh, R. Wisniewski, and S. Kanev. An optimization framework for load and power distribution in wind farms. *Journal of Wind Engineering and Industrial Aerodynamics*, 2012. Accepted for publication.
[22] M. Steinbuch, W.W. de Boer, O.H. Bosora, S.A.W.M. Peters, and J. Ploeg I. Optimal control of wind power plants. *Journal of Wind Engineering and Industrial Aerodynamics*, 27:237–246, 1988.
[23] J. Tzanos, K. Margellos, and John Lygeros. Optimal wind turbine placement via randomized optimization techniques. *NONE*, August 2011.
[24] J.W. Wagenaar, L.A.H. Machielse, and J.G. Schepers. Controlling wind in ECN's scaled wind farm. In *EWEA Conference*, 2012. ECN-M-12-007.
[25] L. Xu and D. Tretheway. Flexible ramping products, 2012. CAISO draft final proposal, April 9.